Bull. Astr. Soc. India (1997) **25**, 353–377

Solar log gf values in the infrared J and H bands

C.S. Stalin, Chetna Trivedi, K. Sinha and B.B. Sanwal

U.P. State Observatory, Manora Peak, Naini Tal 263 129, India

Received 24 March 1997; accepted 10 April 1997

Abstract. Solar IR spectra have been utilized to derive log gf values for atomic lines due to 17 chemical elements. From a recent publication in Astronomy and Astrophysics Supplement, we selected unblended solar lines in the infrared J and H bands, i.e., in the wavelength ranges 1.00 – 1.34 μm and 1.49 – 1.80 μm respectively. The observed central line depths defined by $d = (I_{cont.} - I_{line}) / I_{cont}$, were based on FTS atlases published at Liège and Kitt Peak National Observatory. The observed central line depths were fitted with the corresponding quantities in the calculated spectrum obtained using computer codes and a reliable solar model atmosphere. This provided us with a set of relative log gf values which we present here. Significant differences are noticed between the derived log gf values and those available in literature.

Key words : Sun : atmosphere - Sun : abundances - atomic data

1. Introduction

Among other things, the strength of a Fraunhofer line depends upon the number of absorbers producing the line and its oscillator strength. Therefore, in order to determine the abundances of the elements, a precise knowledge of weighted oscillator strengths (gf) is necessary. The entire edifice of our knowledge of the chemical abundances of celestial bodies depends upon the accuracy of the gf values. Great efforts have been put in by theoretical and experimental physicists as well as by astrophysicists for a reliable estimate of these parameters.

Theoretical gf values in the infrared region of the spectrum have been calculated for large number of atomic lines by Biémont & Grevesse (1973) and KP (Kurucz & Peytremann 1975). Improvements upon the calculations of KP were made by Kurucz (1994) to provide data for about 58 million lines. An important breakthrough in experimental techniques have been made by Professor Blackwell and his group at Oxford (Blackwell *et al.* 1976, 1979 a, b, 1980, 1982 a, b, c, d). The OP (The Opacity Project 1995) and the OPAL (Rogers & Iglesias 1995) projects too have contributed to a huge quantity of data needed to compute opacities in stellar

atmospheres. In spite of these and several other great efforts and because of the daunting nature of the work involved, gf values are still lacking for a large number of Fraunhofer lines, especially for weak lines that are important to astrophysicists.

The importance of weak transitions in the determination of interstellar and cosmic abundances has been described e.g. by Keenan *et al.* (1990). Under such circumstances astrophysical methods of gf determinations particularly those based on the solar spectra come in handy. These values are important because they are still sometimes the only available values, especially for weak lines and are often more reliable than the measured ones (Blackwell 1990).

Gurtovenko & Kostik (1981, 1982, 1989; hereinafter GK) and Thévenin (1989, 1990) have used the solar spectrum in the optical region to derive solar log gf values for a large number of atomic lines. In the earlier attempts, perhaps because of the lack of solar atlases in the IR region of the spectrum, a similar effort could not be taken up. Recent developments in astronomical techniques and instrumentation have made available high resolution solar FTS atlases such as Liège-81 (Delbouille *et al.* 1981), KPNO-91 (Livingston & Wallace 1991), KPNO-93 (Wallace *et al.* 1993) and KPNO-94 (Wallace et al. 1994) which may be used for a work similar to that of GK and Thévenin (1989, 1990). Described in the following sections are our motivation for the present work, the method employed and a discussion of the results.

2. Motivation and method of calculation

Based on the Liège-81, KPNO-91 and KPNO-93 atlases, Solanki et al. (1990) and RSB (Ramsauer *et al.* 1995) have tabulated a large list of interesting lines in the infrared solar spectrum between 1.0 and 1.8 μm. These authors have also tabulated the log gf values for the infrared lines taken from Biémont & Grevesse (1973), KP (Kurucz & Peytremann, 1975), Kurucz (1991), Biémont *et al.* (1994) and Nave *et al.* (1994). Recently, we successfully employed GK's method to derive the log gf values from the solar spectrum in the wavelength range $\lambda\lambda$ 6209 - 6273 Å for use in interpreting the spectrum of the star γ Draconis (Stalin *et al.* 1996; hereinafter referred to as paper I). This prompted us to derive solar log gf values for a comparison with the values tabulated by RSB. Such a comparison should illustrate whether GK's method can be extended to the IR lines as well and if so, we might eventually get better estimates of log gf at least in certain cases.

In our initial efforts, we chose all the lines in J and H bands for which log gf values are available (Tables 1 and 3 of RSB). However, the lines that are blended with other solar lines were dropped from the list. Also dropped are the lines superscripted α in RSB tables. We found that additional solar lines in the neighbourhood of lines selected by us are already identified in KPNO - 91 and for which log gf values may or may not be available in literature. These lines too were included in the calculations.

We have closely followed our Paper I and GK for the derivation of the log gf from the solar spectra. The underlying assumption is that the programme must iterate on log gf until a satisfying agreement between the calculated and the observed absorption peaks is found. Significant differences noticed between the compiled and the derived values may indicate

problems associated with the atomic data, with the purity and the identification of the lines and / or with the suitability of the line for such an analysis.

Particular emphasis upon the technique utilized by GK and followed by us, has been laid by Führ (1987) and by Blackwell (1990). They state that the use of equivalent widths or central line depths taken from the Liège atlas (Delbouille et al. 1973) in combination with the HM photospheric model (Holweger & Müller 1974) provides log gf values which are accurate to within 50%. We have adopted the procedure of line depth fit, since the central depths are expected to be less blended in comparison to line profiles and equivalent widths. The KPNO atlases give lines relatively free of telluric blends when compared to the Liège atlas, but at the cost of a lower resolution and a lower signal - to - noise ratio. The histogram of Fig. 1a shows the distribution of line quality for Liège lines as given by RSB and used in our analysis, and Fig. 1b shows the same for the KPNO lines. A comparison of the two histograms show that KPNO lines are better than Liège lines.

The solar spectrum was generated by us under the assumption of LTE utilizing the computer code ADRSL. It derives from a program originally written in ALGOL by Baschek *et al.* (1966). This program was translated into FORTRAN by Peytremann *et al.* (1967). Details on the procedures and equations used can be found in the original paper by Baschek *et al.* (1966) as well as in Chmielewski (1979). The input list of abundances are taken from Anders & Grevesse (1989) and Grevesse & Noels (1993). For these abundances, the gas pressures and the electron pressures were recalculated by us as functions of the optical depth using the HM model atmosphere. The spectrum was convolved with a depth independent gaussian macroturbulence V_{macro} = 1.52 kms^{-1}. A depth independent microturbulence was assumed : V_{micro} = 1.00 kms^{-1}. Hyperfine splitting was not taken into account and the van der Waals' broadening was calculated from Unsöld's (1955) formulae. Monochromatic continuous opacities are calculated by the program ATM a part of the ADRSL code. In that way, we could obtain solar log gf values for 17 chemical elements.

3. Discussion of the results

The relative log gf values derived are given in Tables 1 and 2. The accuracy of the solar values depends upon the uncertainties affecting following factors :

3.1 Adopted photospheric model and the computer code,
3.2 Choice of the microturbulence velocity, V_{micro},
3.3 Accuracy of the observations,
3.4 Choice of the large scale velocity field, V_{macro},
3.5 Exact location of the continuum and
3.6 Choice of the damping constant.

Points 3.1 and 3.2 are very well discussed in GK and in Paper I and point 3.3 has been covered by RSB. So they need not be repeated here, but at the same time we draw attention to the fact that different central depths for one and the same line in the Liège and the KPNO atlases were noticed by us.

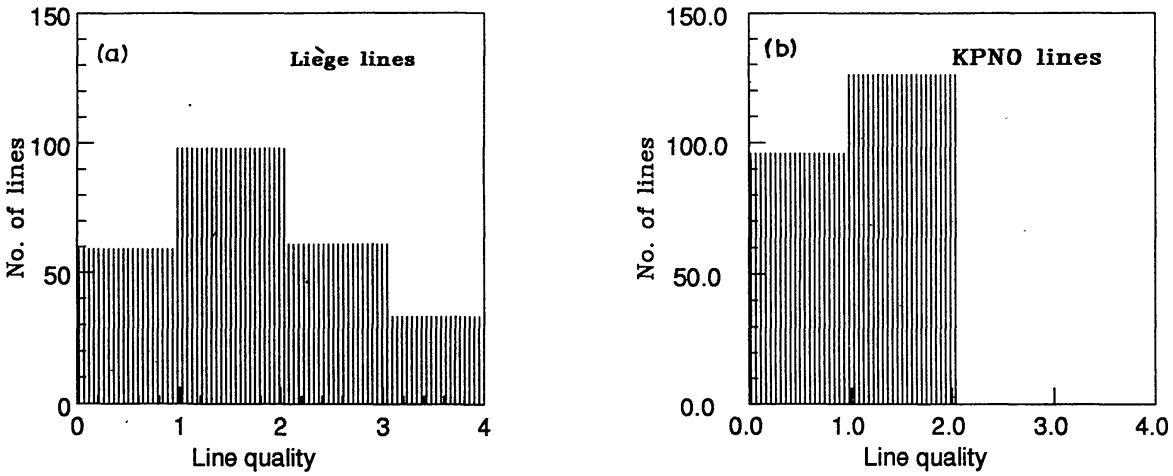

Figure 1a. Distribution of the quality of the lines for the Liège atlas as listed by RSB and used in our analysis. **b.** Same as in Fig. 1a, but for the KPNO atlas.

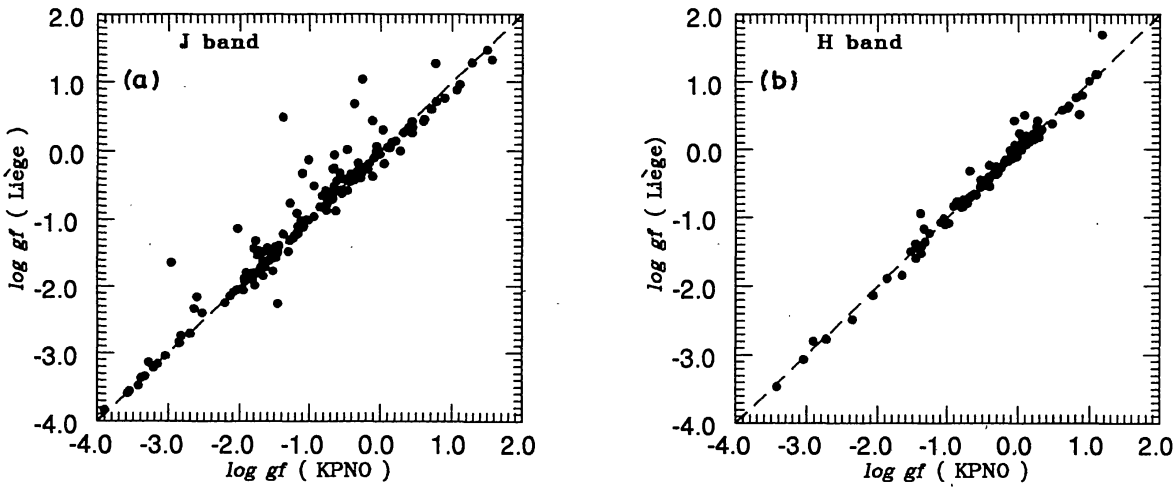

Figure 2a. Comparison of the log gf values derived using the Liège and KPNO atlases respectively for the J band lines. **b.** Same as in Fig. 2a, but for the H band lines.

3.4 Choice of the large scale velocity field V_{macro} : Line depth fits are sensitive to the macroturbulence. To estimate the uncertainties we have recomputed log gf after changing V_{macro} by ± 0.1 kms^{-1}. Figures 3 and 4 demonstrate the effect of macroturbulence on the log gf derived, plotted against the lower excitation potential and central depths of the lines. Our results show that a change of ± 0.1 kms^{-1} produces only 0.01 to 0.04 dex change in log gf. The large change of 0.04 dex occurs in the case of large central depth lines as well as lines of medium excitation potential. From these figures we feel that a precise value of V_{macro} is not very important for weak lines.

3.5 Exact location of the continuum : In the Liège atlas, in order to bring the continuum to unity, a continuum 1% below the one indicated in the atlas was used whereas in the KPNO atlases, the continuum marked in the atlases were used to define the central line depths.

To estimate the uncertainties in log gf values introduced by a selective location of the continuum, the continuum was varied by ± 1% in the atlases. The differences in log gf thus obtained are plotted as functions of the central depths in Fig. 5 and Fig. 6 for the Liège and the KPNO atlases respectively. As it can be expected, the weak and strong lines are affected most. For a large number of lines with moderate central depths, the differences remain within 25% of the uncertainty, but for lines with large central depths the uncertainty is as large as 60%. For strong lines with a large central depth LTE does not seem to be a valid criterion (cf. GK).

3.6 Choice of damping constants : The intensities in the line wings are controlled by the parameter γ_6, obtained from the formulae given by Unsöld (1955). It has been a subject of discussion how accurate the factors thus obtained are. Various laboratory measurements, theoretical predictions and empirical determinations have shown that γ_6 tends to exceed this estimate (Kostik *et al.* 1996). Different enhancement factors for the same parameter have been used by different authors. Following Holweger *et al.* (1990) and Holweger *et al.* (1991) for the Fe I and Fe II lines we used logarithm of enhancement factors equal to 0.75 and 1.00 respectively. The advantage of the line depth fit method is that they are practically insensitive to the adopted damping parameter (Kostik et al. 1996). An effort was made to estimate the effect of damping on the derived log gf by repeating the calculations with an enhancement factor equal to 1.5, 2.5 and 3.5. The results are presented in Fig. 7 and Fig. 8 for the Liège and the KPNO atlases respectively. It may be noticed from these figures, that as the line strengths increase, the differences have a tendency to vanish and the weak lines are in general affected in a small way.

The sources of error which we have mentioned above need not be cumulative; they may compensate for each other.

As stated earlier, it was found that, in the KPNO-91 atlas several lines close to those chosen by us are already identified but are not tabulated by RSB. The log gf values for these lines too were derived by us and are presented in Table 2. Wherever possible, in the same table are listed for comparison the log gf as available in the literature. These additional lines have been included in all the figures.

Table 1. Derived log gf values using Liege and KPNO atlases

Wavelength (Laboratory) Å	Element	Lower Excitation Potential (eV)	Central line Depths		RSB	log gf values Present study	
			Liège	KPNO		Liège	KPNO
J band							
10003.099	Ti I	2.16	0.0339		-1.140	-1.222	
10011.824	Ti I	2.15	0.0315		-1.260	-1.265	
10019.792	Fe I	5.48	0.0645		-1.600	-1.308	
10022.287	Fe I	5.51	0.0392		-2.670	-1.528	
10032.858	Fe I	5.51	0.0768		-1.790	-1.190	
10034.480	Ti I	1.46	0.0434		-2.000	-1.790	
10036.660	SrII	3.04	0.4563		-1.310	0.489	
10061.276	Ni I	5.49	0.0428		-0.610	-0.572	
10065.045	Fe I	4.84	0.4663		-2.100	-0.299	
10070.519	Fe I	5.51	0.0519		-1.800	-1.396	
10080.437	Fe I	5.10	0.0371		-2.960	-1.951	
10081.394	Fe I	2.42	0.0533		-4.350	-4.375	
10089.775	Fe I	5.45	0.0500		-1.600	-1.474	
10123.870	C I	8.54	0.2664		-0.330	-0.139	
10137.102	Fe I	5.09	0.0600		-1.700	-1.712	
10149.078	Fe I	5.10	0.0243		-2.090	-2.136	
10155.165	Fe I	2.18	0.1743		-4.230	-4.216	
10193.228	Ni I	4.09	0.3128		-0.790	-0.750	
10195.108	Fe I	2.73	0.1641		-3.700	-3.520	
10216.314	Fe I	4.73	0.5191		-0.220	0.027	
10218.410	Fe I	3.07	0.2779		-2.760	-2.830	
10265.220	Fe I	2.22	0.0590		-4.470	-4.530	
10288.940	Si I	4.92	0.3734		-1.360	-1.699	
10301.380	Si I	6.10	0.0580		-1.660	-1.824	
10302.611	Ni I	4.27	0.1682		-1.070	-1.056	
10307.454	Fe I	4.59	0.0422		-2.110	-2.389	
10330.246	Ni I	4.11	0.1929		-1.230	-1.054	
10332.329	Fe I	3.64	0.0740		-2.940	-3.048	
10340.886	Fe I	2.20	0.3256	0.3223	-3.490	-3.554	-3.555
10343.820	Ca I	2.93	0.5381	0.5392	-0.410	0.049	0.129
10347.966	Fe I	5.39	0.2120	0.2131	-0.800	-0.758	-0.747
10362.704	Fe I	5.48	0.0714	0.0784	-2.470	-1.280	-1.228
10364.062	Fe I	5.45	0.1041	0.1094	-1.210	-1.119	-1.088
10371.269	Si I	6.12	0.5394	0.5435	-0.640	0.763	0.888
10378.623	Ni I	4.09	0.2928	0.2955	-0.970	-0.819	-0.800
10388.744	Fe I	5.45	0.0486	0.0527	-1.300	-1.493	-1.451
10395.797	Fe I	2.18	0.3984	0.3961	-3.330	-3.340	-3.334
10396.850	Ti I	0.85	0.1854	0.1865	-1.540	-1.686	-1.675
10423.030	Fe I	2.69	0.1578	0.1585	-3.780	-3.587	-3.578
10423.745	Fe I	3.07	0.2075	0.2063	-2.920	-3.045	-3.042

Table 1. (continued)

Wavelength (Laboratory) Å	Element	Lower Excitation Potential (eV)	Central line Depths Liège	Central line Depths KPNO	RSB	log gf values Present study Liège	log gf values Present study KPNO
10456.790	S I	6.86	0.2536	0.2563	-0.420	-0.568	-0.544
10459.460	S I	6.86	0.3730	0.3764	0.060	0.051	0.094
10469.654	Fe I	3.88	0.4587	0.4602	-1.230	-1.316	-1.279
10486.212	Cr I	3.01	0.1691	0.1730	-0.970	-1.104	-1.084
10496.084	Ti I	0.84	0.1560	0.1576	-1.650	-1.801	-1.790
10511.584	P I	6.94	0.0368	0.0433	-0.100	-0.266	-0.178
10529.522	P I	6.95	0.0762	0.0797	0.270	0.121	0.152
10530.531	Ni I	4.11	0.1612	0.1659	-1.190	-1.239	-1.216
10532.236	Fe I	3.93	0.3747	0.3723	-1.530	-1.660	-1.655
10555.651	Fe I	5.45	0.0741	0.0768	-1.690	-1.296	-1.273
10577.141	Fe I	3.30	0.1166	0.1171	-3.270	-3.160	-3.153
10581.569	P I	6.99	0.1107	0.1123	0.490	0.424	0.437
10582.150	Si I	6.22	0.1667	0.1684	-1.010	-1.172	-1.161
10596.900	P I	6.94	0.0379	0.0376	-0.170	-0.255	-0.255
10611.714	Fe I	6.17	0.1851	0.1845	-0.340	-0.055	-0.045
10616.723	Fe I	3.27	0.1109	0.1095	-3.260	-3.213	-3.213
10672.158	Cr I	3.01	0.0892	0.0865	-1.370	-1.446	-1.456
10685.350	C I	7.48	0.4261	0.4255	-0.290	-0.188	-0.160
10689.720	Si I	5.95	0.5143	0.5139	-0.190	0.337	0.390
10694.251	Si I	5.96	0.5363	0.5383	-0.060	0.604	0.703
10707.330	C I	7.48	0.3963	0.3988	-0.390	-0.403	-0.357
10727.410	Si I	5.98	0.5544	0.5606	0.060	0.883	1.064
10729.530	C I	7.49	0.3920	0.3973	-0.340	-0.422	-0.358
10753.007	Fe I	3.96	0.2483	0.2516	-1.900	-2.054	-2.036
10762.273	Ni I	4.15	0.0396	0.0480	-2.000	-1.913	-1.815
10780.694	Fe I	3.24	0.0683	0.0754	-3.410	-3.477	-3.429
10783.051	Fe I	3.11	0.3054	0.3060	-2.600	-2.714	-2.704
10784.550	Si I	5.96	0.3603	0.3656	-0.910	-0.710	-0.670
10801.346	Cr I	3.01	0.0517	0.0593	-1.720	-1.710	-1.640
10818.276	Fe I	3.96	0.2174	0.2191	-2.000	-2.152	-2.139
10838.970	Ca I	4.88	0.1388	0.1468	-0.030	1.472	1.495
10843.850	Si I	5.86	0.5316	0.5377	-0.310	0.457	0.606
10846.792	Ca I	4.74	0.0457	0.0538	-1.140	-0.619	-0.540
10849.467	Fe I	5.54	0.2139	0.1989	-1.830	-0.613	-0.658
10861.582	Ca I	4.88	0.0507	0.0559	-0.610	-0.292	-0.246
10862.644	FeII	5.59	0.0762	0.0825	-2.120	-2.253	-2.209
10879.868	Ca I	4.88	0.0469	0.0537	-0.620	-0.328	-0.260
10881.760	Fe I	2.85	0.1782	0.1694	-3.710	-3.366	-3.390
10882.802	Si I	5.98	0.3597	0.3621	-0.870	-0.686	-0.665
10884.265	Fe I	3.93	0.2431	0.2441	-1.970	-2.088	-2.084

Table 1. (continued)

Wavelength (Laboratory) Å	Element	Lower Excitation Potential (eV)	Central line Depths Liège	Central line Depths KPNO	RSB	log gf values Present study Liège	log gf values Present study KPNO
10885.330	Si I	6.18	0.4652	0.4689	0.040	0.143	0.207
10896.302	Fe I	3.07	0.2720	0.2716	-2.730	-2.856	-2.849
10914.230	MgII	8.86	0.1897	0.1945	0.020	-0.047	-0.012
10951.790	MgII	8.86	0.1469	0.1405	-0.230	-0.300	-0.330
10982.060	Si I	6.19	0.4458	0.4342	-0.050	0.011	-0.035
11015.620	Cr I	3.45	0.2524	0.2191	-2.360	-0.408	-0.508
11119.798	Fe I	2.85	0.4735	0.5538	-2.200	-2.267	-1.453
11308.480	Si I	6.19	0.3387	0.2896	-0.790	-0.577	-0.766
11388.540	Fe I	5.62	0.1820	0.1549	-0.710	-0.652	-0.748
11390.749	Cr I	3.32	0.4051	0.2748	-0.490	0.019	-0.469
11422.323	Fe I	2.20	0.5431	0.5078	-2.700	-2.339	-2.645
11465.320	Si I	6.21	0.4213	0.2171	-2.430	-0.126	-1.016
11522.214	Fe I	3.24	0.4997	0.1885	-3.410	-1.641	-2.961
11588.712	Ni I	4.24	0.1391	0.1052	-1.430	-1.219	-1.375
11591.510	Si I	6.27	0.4043	0.4336	-0.900	-0.183	0.049
11592.390	Si I	6.27	0.4052	0.3754	-1.050	-0.172	-0.314
11593.591	Fe I	2.22	0.6312	0.5600	-2.450	-1.134	-2.032
11607.575	Fe I	2.20	0.5708	0.5803	-2.010	-1.986	-1.782
11619.290	C I	8.64	0.2229	0.1743	-0.500	-0.318	-0.568
11627.530	Si I	5.96	0.0989	0.1500	-2.880	-1.770	-1.521
11628.830	C I	8.64	0.3493	0.2569	-0.090	0.435	-0.118
11640.982	Si I	6.27	0.3623	0.3823	-0.950	-0.398	-0.275
11647.994	C I	8.64	0.1494	0.1490	-0.990	-0.728	-0.723
11659.677	C I	8.65	0.2790	0.3201	0.100	0.001	0.271
11753.315	C I	8.65	0.3861	0.3891	0.690	0.713	0.770
11754.766	C I	8.64	0.4524	0.3891	0.440	1.272	0.760
11801.080	C I	8.65	0.2699	0.1594	-2.390	-0.059	-0.649
11838.997	CaII	6.47	0.5294	0.5233	0.280	1.283	1.277
11848.721	C I	8.64	0.1459	0.1571	-0.680	-0.702	-0.682
11862.992	C I	8.64	0.1426	0.1466	-0.740	-0.781	-0.749
11863.935	Si I	5.98	0.1720	0.1641	-2.730	-1.432	-1.456
11882.847	Fe I	2.20	0.5994	0.5976	-1.670	-1.575	-1.514
11884.085	Fe I	2.22	0.5612	0.5642	-2.080	-2.064	-1.948
11890.490	Fe I	5.54	0.2928	0.2910	-0.420	-0.378	-0.374
11895.741	C I	8.65	0.2634	0.2616		-0.101	-0.097
11900.055	Si I	5.96	0.1529	0.1034	-2.610	-1.528	-1.746
11949.745	CaII	6.47	0.4379	0.4456	-0.020	0.340	0.440
11955.955	Ca I	4.13	0.1048	0.1185	-0.140	-0.876	-0.625
11973.050	Fe I	2.18	0.7359	0.6161	-1.480		-1.262
12039.820	Mg I	5.75	0.2306	0.2204	-2.330	-1.596	-1.576

Table 1. (continued)

Wavelength (Laboratory) Å	Element	Lower Excitation Potential (eV)	Central line Depths Liège	Central line Depths KPNO	RSB	log gf values Present study Liège	log gf values Present study KPNO
12053.083	Fe I	4.56	0.2066	0.2192	-1.540	-1.619	-1.570
12080.391	Si I	6.26	0.0779	0.1040	-2.230	-1.845	-1.662
12105.841	Ca I	4.55	0.0937	0.1034	-1.840	-0.599	-0.549
12119.495	Fe I	4.59	0.1851	0.1887	-2.020	-1.680	-1.667
12175.749	Si I	6.62	0.1241	0.1223	-2.820	-1.009	-1.011
12190.099	Fe I	3.64	0.3248	0.1854	-2.330	-2.163	-2.606
12213.333	Fe I	4.64	0.1099	0.1107	-1.950	-1.938	-1.928
12227.113	Fe I	4.61	0.2444	0.2404	-1.460	-1.569	-1.476
12270.693	Si I	4.95	0.5764	0.5811	-0.410	0.261	0.437
12314.086	C I	9.71	0.0493	0.0592	-0.070	-0.577	-0.461
12342.914	Fe I	4.64	0.1969	0.2225	-1.560	-1.581	-1.516
12390.165	Si I	5.08	0.3122	0.3198	-1.870	-1.829	-1.790
12395.834	Si I	4.95	0.3684	0.3704	-1.630	-1.731	-1.705
12417.929	Mg I	5.93	0.1419	0.1620	-1.660	-1.714	-1.629
12423.029	Mg I	5.93	0.2803	0.2911	-1.180	-1.216	-1.165
12432.244	K I	1.61	0.1975	0.2096	-0.460	-0.372	-0.323
12460.616	Ti I	4.24	0.0585	0.0777	-2.400	0.963	1.108
12510.519	Fe I	4.96	0.0739	0.0730	-1.650	-1.841	-1.842
12532.838	Cr I	2.71	0.0884	0.0684	-1.870	-1.790	-1.906
12549.480	C I	8.85	0.1638	0.1417	-1.010	-0.522	-0.649
12556.999	Fe I	2.28	0.2242	0.2005	-3.630	-3.832	-3.899
12583.977	Si I	6.62	0.2579	0.2188	-1.010	-0.518	-0.650
12601.489	C I	8.85	0.2132	0.1422	-0.890	-0.249	-0.652
12615.926	Fe I	4.64	0.2377	0.1779	-1.600	-1.486	-1.666
12638.706	Fe I	4.56	0.4697	0.4010	-0.860	-0.509	-0.933
12648.742	Fe I	4.61	0.4272	0.3081	-1.140	-0.760	-1.273
12679.145	Na I	3.62	0.3633	0.3100	-0.040	0.304	0.031
12749.906	Al I	4.02	0.0852	0.0500	-2.210	-1.467	-1.723
12807.150	Fe I	3.64	0.2577	0.2151	-2.520	-2.402	-2.531
12808.244	Fe I	4.99	0.1593	0.1133	-1.540	-1.421	-1.604
12831.437	Ti I	1.43	0.1284	0.1163	-1.550	-1.391	-1.436
12840.574	Fe I	4.96	0.1470	0.1340	-1.500	-1.496	-1.543
12847.029	Ti I	1.44	0.1214	0.1029	-1.430	-1.408	-1.484
12896.119	Fe I	4.91	0.1213	0.1112	-1.580	-1.623	-1.665
12909.070	Ca I	4.43	0.1503	0.1560	-0.430	-0.449	-0.421
12910.089	Cr I	2.71	0.0881	0.0938	-1.750	-1.813	-1.777
12932.327	Ni I	2.74	0.1112	0.1061	-3.900	-2.839	-2.857
12933.006	Fe I	5.02	0.0741	0.0706	-1.730	-1.801	-1.819
12934.667	Fe I	5.39	0.1419	0.1267	-0.820	-1.103	-1.161
12937.018	Cr I	2.71	0.0764	0.0674	-1.890	-1.881	-1.936

Table 1. (continued)

Wavelength (Laboratory) Å	Element	Lower Excitation Potential (eV)	Central line Depths		RSB	log gf values Present study	
			Liège	KPNO		Liège	KPNO
13006.688	Fe I	2.99	0.2293	0.1818	-4.120	-3.137	-3.282
13014.842	Fe I	5.45	0.0640	0.0607	-1.750	-1.463	-1.483
13029.573	Si I	6.08	0.2041	0.2132	-2.410	-1.276	-1.235
13030.966	Si I	6.08	0.3642	0.3246	-2.400	-0.652	-0.817
13033.555	Ca I	4.44	0.2139	0.2194	-0.270	-0.213	-0.186
13039.652	Fe I	5.66	0.2903	0.0862	-2.400	-0.326	-1.100
13098.876	Fe I	5.01	0.1546	0.1139	-1.480	-1.432	-1.590
13134.942	Ca I	4.45	0.2930	0.2551	-0.120	0.065	-0.058
13147.922	Fe I	5.39	0.2659	0.2498	-1.080	-0.682	-0.728
13154.530	Si I	6.62	0.1174	0.1049	-2.680	-1.102	-1.159
13176.906	Si I	5.86	0.5093	0.5081	-0.500	0.265	0.317
13201.144	Cr I	2.71	0.1830	0.0852	-1.820	-1.434	-1.799
13212.458	Ni I	2.74	0.1357	0.1151	-2.580	-2.747	-2.827
13291.786	Fe I	5.48	0.4752	0.0691	-1.920	0.487	-1.383
13293.795	Mn I	2.14	0.4387	0.4204	-1.610	-1.430	-1.456
13317.984	Ca I	4.62	0.1415	0.0718	0.560	-0.265	-0.670
13319.068	Mn I	2.14	0.5077	0.4728	-1.620	-0.909	-1.177
H Band							
14929.151	Fe I	5.48	0.1948	0.0871	-2.000	-0.938	-1.390
15120.509	Fe I	5.45	0.1455	0.1042	-0.800	-1.161	-1.342
15122.382	Fe I	5.62	0.3093	0.3165	-0.380	-0.449	-0.413
15173.585	Ni I	5.49	0.0574	0.0590	-0.690	-0.701	-0.684
15176.717	Fe I	5.92	0.1129	0.1212	-1.260	-0.847	-0.802
15194.492	Fe I	2.22	0.0655	0.0711	-4.780	-4.682	-4.632
15207.530	Fe I	5.39	0.4789	0.4857	0.210	0.178	0.289
15219.622	Fe I	5.59	0.4190	0.4206	-0.820	-0.037	-0.004
15243.590	Si I	6.73	0.0719	0.0778	-0.600	-1.420	-1.375
15244.973	Fe I	5.59	0.4156	0.4150	-0.090	-0.058	-0.039
15343.802	Fe I	5.65	0.2302	0.2354	-0.690	-0.684	-0.660
15361.160	Si I	5.95	0.0770	0.0864	-1.990	-2.131	-2.068
15469.800	S I	8.05	0.1254	0.1304	-0.220	-0.505	-0.468
15534.247	Fe I	5.64	0.3327	0.3353	-0.420	-0.368	-0.347
15543.680	Ti I	1.88	0.0753	0.0792	-1.220	-1.357	-1.324
15593.752	Fe I	5.03	0.0827	0.0857	-2.090	-1.890	-1.867
15611.138	Fe I	3.42	0.1597	0.1650	-3.890	-3.065	-3.042
15621.659	Fe I	5.54	0.4849	0.4891	-0.360	0.379	0.473
15648.515	Fe I	5.43	0.2926	0.2983	-0.670	-0.712	-0.683
15723.593	Fe I	5.62	0.4375	0.4362	-0.140	0.083	0.103

Table 1. (continued)

Wavelength (Laboratory) Å	Element	Lower Excitation Potential (eV)	Central line Depths		RSB	log gf values Present study	
			Liège	KPNO		Liège	KPNO
15822.821	Fe I	5.64	0.4785	0.4043	0.070	0.424	-0.058
15868.526	Fe I	5.59	0.4025	0.4077	0.050	-0.139	0.091
15901.520	Fe I	5.92	0.2080	0.2154	-0.530	-0.502	-0.470
15911.304	Fe I	5.87	0.3487	0.3538	-1.800	0.066	0.053
15928.168	Fe I	5.95	0.1163	0.1236	-0.970	-0.825	-0.785
15960.040	Si I	5.98	0.5351	0.5470	0.130	0.517	0.852
15964.869	Fe I	5.92	0.3296	0.3484	-0.210	-0.106	0.024
16009.615	Fe I	5.43	0.3523	0.3611	-0.550	-0.520	-0.463
16060.024	Si I	5.95	0.4756	0.4677	-0.440	-0.279	-0.306
16094.800	Si I	5.96	0.5233	0.5130	-0.110	0.332	0.258
16150.763	Ca I	4.53	0.2001	0.2061	0.360	-0.340	-0.312
16155.236	Ca I	4.53	0.0899	0.0950	-0.120	-0.822	-0.785
16197.075	Ca I	4.53	0.2987	0.3054	0.640	-0.012	0.019
16198.505	Fe I	5.41	0.3658	0.3694	-0.520	-0.472	-0.442
16241.840	Si I	5.96	0.4038	0.4067	-1.200	-0.790	-0.747
16292.848	Fe I	5.92	0.1919	0.1962	-0.830	-0.551	-0.530
16310.497	Ni I	5.28	0.2540	0.2568	0.070	-0.046	-0.028
16331.529	Fe I	5.98	0.1797	0.1854	-1.330	-0.539	-0.507
16434.930	Si I	5.96	0.2555	0.2293	-1.470	-1.387	-1.467
16436.626	Fe I	5.92	0.2340	0.2334	-0.020	-0.411	-0.405
16444.818	Fe I	5.83	0.4670	0.4653	0.520	0.581	0.611
16468.527	FeII	4.82	0.0508	0.0546	-0.710	-3.462	-3.421
16474.085	Fe I	6.02	0.1834	0.1855	-0.960	-0.476	-0.463
16486.669	Fe I	5.83	0.4855	0.4836	0.720	0.772	0.808
16506.298	Fe I	5.95	0.2261	0.2255	-0.510	-0.404	-0.411
16586.054	Fe I	5.62	0.0658	0.0679	-0.940	-1.449	-1.428
16619.745	Fe I	5.59	0.0637	0.0587	-1.740	-1.495	-1.530
16750.587	Al I	4.09	0.5588	0.5282	0.550	1.698	1.173
16763.366	Al I	4.09	0.3544	0.3532	-0.400	-0.534	-0.524
16815.465	Ni I	5.31	0.1287	0.1192	-0.550	-0.460	-0.498
16820.515	Fe I	5.97	0.2938	0.2819	-1.580	-0.154	-0.185
16828.180	Si I	5.98	0.3342	0.3243	-1.390	-1.071	-1.097
16929.861	Mn I	6.41	0.0594	0.0543	-3.160	1.115	1.078
16945.307	Ni I	5.36	0.0645	0.0602	-1.220	-0.788	-0.817
16957.794	Si I	7.09	0.0522	0.0485	-1.180	-1.228	-1.259
17011.101	Fe I	5.95	0.3158	0.3110	-0.130	-0.092	-0.097
17045.102	Ca I	5.23	0.1160	0.1102	-1.550	0.198	0.174
17108.632	Mg I	5.39	0.5673	0.5658	0.140	0.801	0.892
17120.506	Ni I	6.04	0.0529	0.0360	0.090	-0.231	-0.406
17161.109	Fe I	6.02	0.2649	0.2614	-0.150	-0.190	-0.193

Table 1. (continued)

Wavelength (Laboratory) Å	Element	Lower Excitation Potential (eV)	Central line Depths Liège	Central line Depths KPNO	RSB	log gf values Present study Liège	log gf values Present study KPNO
17205.760	Si I	6.08	0.2148	0.1972	-1.590	-1.392	-1.447
17234.470	C I	9.70	0.1972	0.1807	0.170	0.151	0.061
17306.518	Ni I	5.49	0.0860	0.0844	-0.560	-0.508	-0.511
17327.290	Si I	6.62	0.5019	0.4953	0.730	1.014	0.992
17455.990	C I	9.70	0.2088	0.1708	0.430	0.236	0.014
17522.776	Sc I	4.27	0.2987	0.0809	0.220	3.626	2.766
17538.635	Fe I	5.72	0.1196	0.1102	-1.660	-1.015	-1.054
17768.940	C I	9.71	0.2009	0.1978	0.160	0.224	0.218
17771.126	Fe I	5.95	0.3740	0.3519	0.110	0.201	0.111
17789.655	C I	7.95	0.0893	0.0485	-1.530	-2.484	-2.361
17793.264	C I	9.71	0.5364	0.1143	-1.380		-0.309
17814.030	C I	9.71	0.2464	0.1760	-0.050	0.506	0.089
17826.320	C I	9.71	0.2303	0.2037	-0.510	0.418	0.268

Table 2. Additional lines for which log gf have been derived

Wavelength (Labgratory) Å	Element	Lower Excitation Potential (eV)	Central line Depths Liège	Central line Depths KPNO	log gf values Literature	log gf values Present study Liège	log gf values Present study KPNO
J band							
11594.551	Fe I	4.58	0.2929	0.1613	-2.250*	-1.319	-1.772
11658.849	C I	8.77	0.1922	0.2362	-0.350*	-0.368	-0.112
12082.001	Si I	6.26	0.5065	0.3753	-0.980*	0.683	-0.368
12083.650	Mg I	5.75	0.5870	0.5940	-2.360* 0.500$	1.329	1.564
12103.582	Si I	4.93	0.5890	0.5934	-0.390* -0.340$	0.429	0.594
12110.673	Si I	6.62	0.5033	0.3149	-0.660*	1.040	-0.254
12189.287	Si I	6.62	0.1024	0.1029	-1.490*	-1.122	-1.113
12432.802	Fe I	5.68	0.0404	0.0558	-2.880*	-1.476	-1.303
12433.450	Mg I	5.93	0.3465	0.3486	-0.960* -0.970$	-0.958	-0.933
12581.586	C I	8.85	0.1792	0.1387	-0.700* -0.520$	-0.438	-0.609
12821.673	Ti I	1.46	0.2298	0.2185	-1.500*	-1.002	-1.043
12823.862	Ca I	3.91	0.1880	0.1776	-2.260*	-0.817	-0.848
12824.849	Fe I	3.02	0.2023	0.1913	-3.840*	-3.190	-3.214
12827.021	Ca I	3.91	0.1199	0.1100	-2.740*	-1.087	-1.128
12899.830	Mn I	2.11	0.5131	0.5177	-1.310*	-0.868	-0.757
H Band							
15217.745	Mn I	4.89	0.2110	0.2187	0.580*	0.296	0.328
15224.721	Fe I	5.96	0.1838	0.1925		-0.523	-0.487
15360.229	Fe I	4.26	0.0612	0.0649		-2.768	-2.731
15375.349	Fe I	5.92	0.0732	0.0826		-1.104	-1.031
15519.370	Fe I	6.29	0.1032	0.1095		-0.528	-0.489
15537.699	Fe I	6.32	0.1534	0.1488		-0.270	-0.284
15590.037	Fe I	6.24	0.1331	0.1392		-0.441	-0.409
15602.835	Ti I	2.27	0.0169	0.0224		-1.524	-1.381
15647.404	Fe I	6.33	0.0320	0.0336		-1.080	-1.053
15652.865	Fe I	6.25	0.2263	0.2316		-0.097	-0.072
15819.140	Fe I	6.30	0.2637	0.2717		0.070	0.107
15833.620	Si I	6.22	0.4339	0.4390	-0.660* -0.130$	-0.353	-0.288
15835.175	Fe I	6.30	0.4129	0.4190		0.644	0.704
15840.191	Fe I	6.36	0.1239	0.1358		-0.368	-0.305
15863.719	Fe I	6.26	0.2762	0.2826		0.069	0.099
15864.650	Fe I	6.36	0.0728	0.0828		-0.668	-0.593
15898.028	Fe I	6.31	0.3089	0.3011		0.231	0.215
15899.268	Fe I	6.31	0.1588	0.1656		-0.274	-0.241
15929.465	Fe I	6.31	0.0994	0.1257		-0.540	-0.403
15962.555	Fe I	6.42	0.2019	0.2188		-0.009	0.044

Table 2. (continued)

Wavelength (Laboratory) Å	Element	Lower Excitation Potential (eV)	Central line Depths Liège	Central line Depths KPNO	log gf values Literature	log gf values Present study Liège	log gf values Present study KPNO
15967.654	Fe I	6.37	0.2968	0.3073		0.254	0.299
16006.744	Fe I	6.35	0.3974	0.4081		0.612	0.687
16007.078	Fe I	6.35	0.2914	0.3045		0.109	0.155
16012.847	Fe I	5.59	0.0309	0.0474		-1.843	-1.653
16039.847	Fe I	5.65	0.0614	0.0763		-1.594	-1.456
16040.647	Fe I	5.87	0.4014	0.4113		0.143	0.216
16100.269	Fe I	6.35	0.2440	0.2152		0.062	0.009
16153.234	Fe I	5.35	0.4130	0.3237		-0.317	-0.677
16156.550	Fe I	5.96	0.2166	0.2219		-0.434	-0.409
16157.357	Ca I	4.55	0.2170	0.2211	-0.160* -0.170$	-0.265	-0.244
16195.049	Fe I	6.39	0.2735	0.2802		0.204	0.235
16201.505	Fe I	6.38	0.0932	0.0978		-0.499	-0.467
16240.879	Fe I	6.32	0.0559	0.0628		-0.844	-0.778
16243.070	Fe I	6.28	0.0377	0.0467		-1.082	-0.980
16245.762	Fe I	6.32	0.0629	0.0713		-0.794	-0.716
16246.450	Fe I	6.28	0.1937	0.1994		-0.177	-0.149
16316.160	Fe I	6.28	0.4760	0.4692		1.113	1.102
16318.688	Fe I	5.92	0.2031	0.2071		-0.521	-0.500
16333.137	Fe I	5.64	0.0625	0.0675		-1.464	-1.418
16440.389	Fe I	6.29	0.1835	0.1845		-0.196	-0.186
16466.926	Fe I	6.39	0.2464	0.2461		0.118	0.127
16476.939	Fe I	6.29	0.1134	0.1085		-0.484	-0.503
16584.443	Ni I	5.31	0.0912	0.0965		-0.657	-0.621
16685.529	Fe I	6.34	0.1306	0.1311		-0.349	-0.341
16723.266	Fe I	5.92	0.2352	0.2323	-0.220*	-0.404	-0.406
16753.055	Fe I	6.38	0.2728	0.2725		0.165	0.199
16822.688	Fe I	6.28	0.0600	0.0508		-0.832	-0.910
17005.455	Fe I	6.07	0.3017	0.2704		-0.018	-0.116
17008.982	Fe I	6.62	0.0968	0.0951		-0.195	-0.199
17037.797	Fe I	6.39	0.1277	0.1242		-0.300	-0.310
17052.182	Fe I	6.39	0.0966	0.0845		-0.450	-0.527
17520.227	Fe I	4.28	0.0564	0.0442		-2.801	-2.911
17524.279	Fe I	6.00	0.1196	0.1107		-0.736	-0.771
17534.730	Fe I	6.64	0.0817	0.0719		-0.253	-0.314
17536.883	Fe I	5.91	0.1326	0.1104		-0.766	-0.865

* means a reference to Biemont & Grevesse (1973)
$ means a reference to Kurucz & Peytremann (1975)

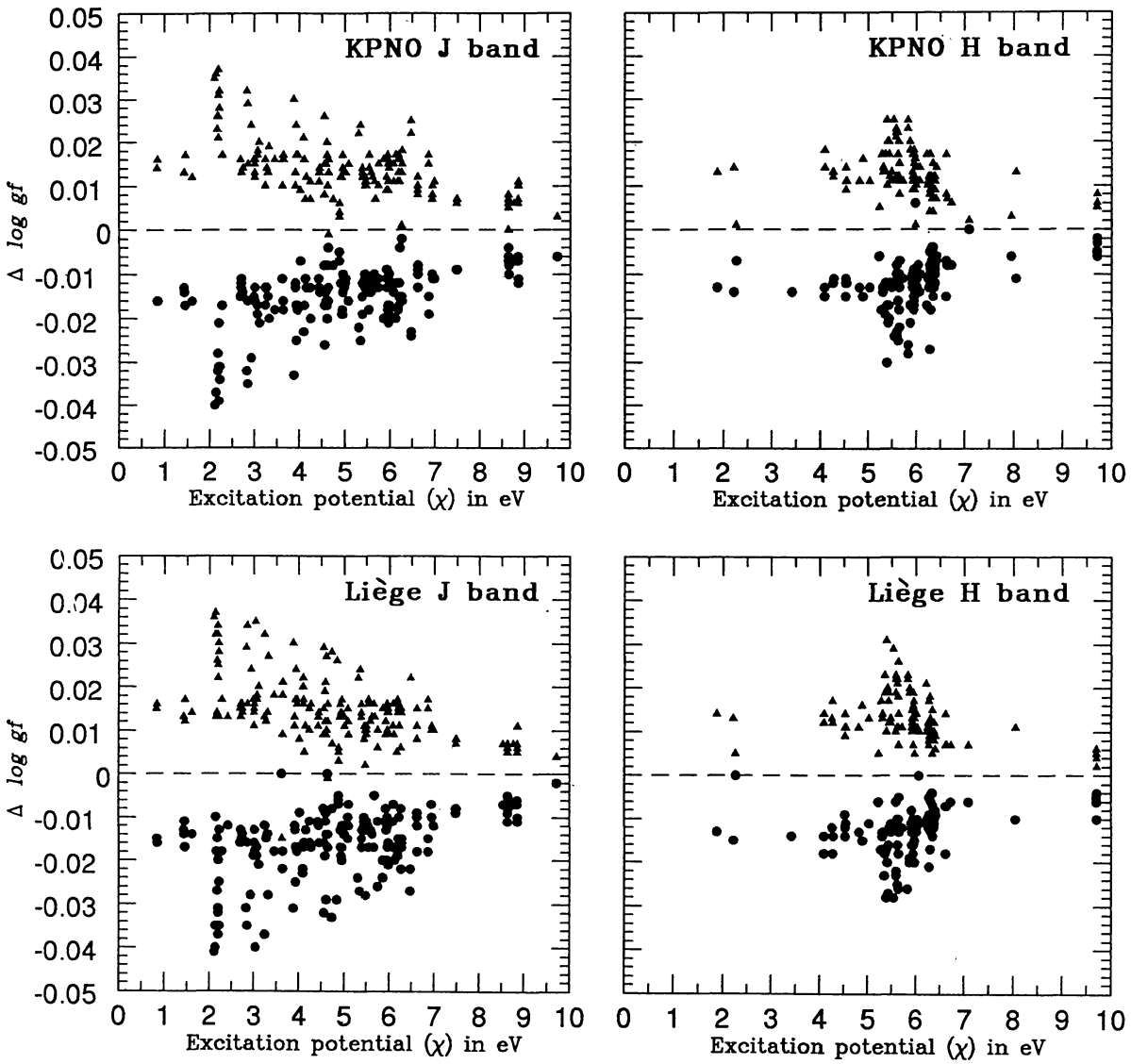

Figure 3. Log gf changes (Δ log gf) against lower excitation potential for the KPNO and Liege atlases respectively due to ± 0.1 kms^{-1} change of the macroturbulence. Filled circle : log gf (1.52 V_{macro}) – log gf (1.62 V_{macro}), Filled triangle : log gf (1.52 V_{macro}) – log gf (1.42 V_{macro}). The top panels are for the KPNO J and H bands and the bottom panels are respectively for the Liege J and H bands.

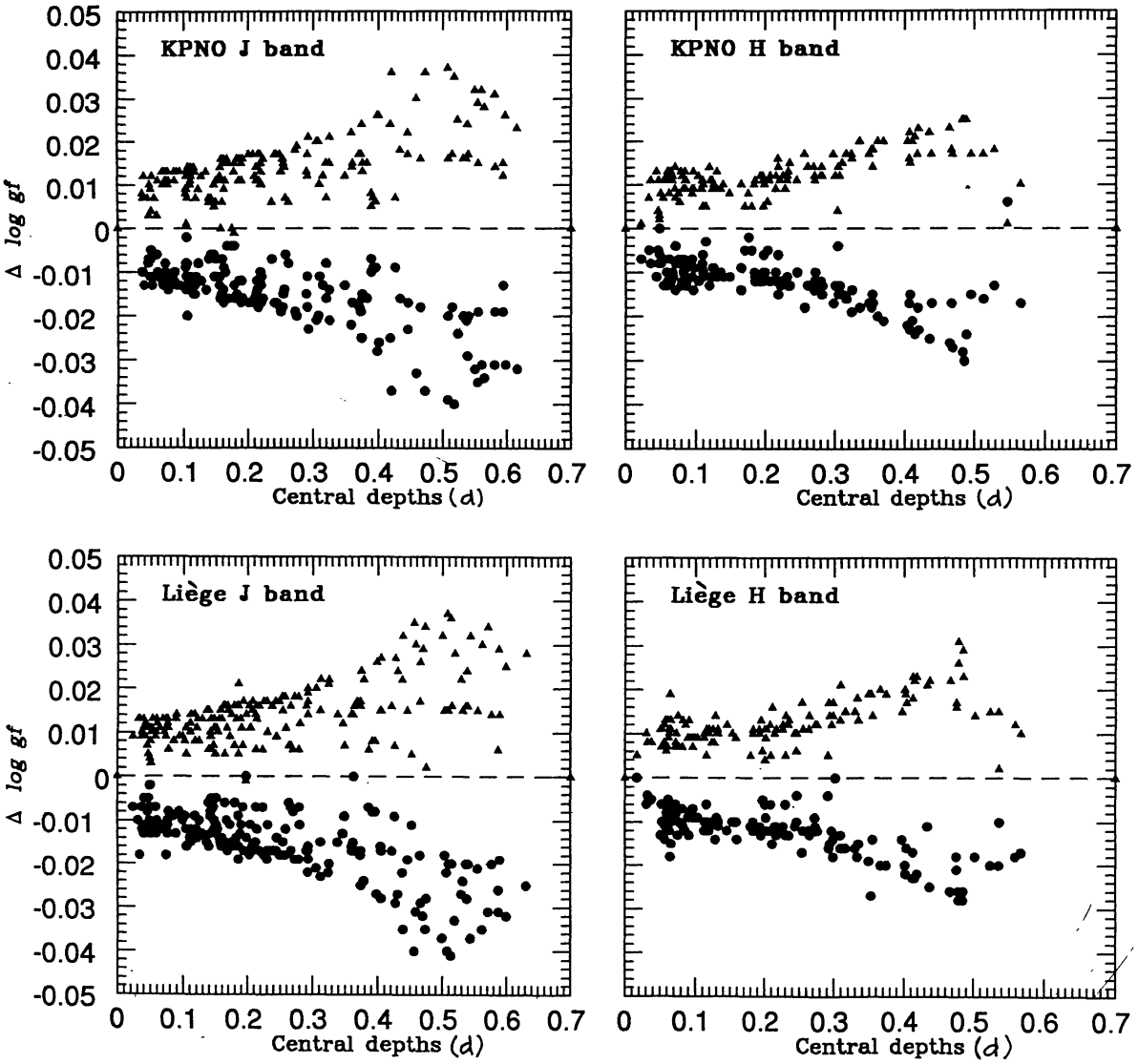

Figure 4. Log gf changes (Δ log gf) against observed central line depths (d) for the KPNO and Liège atlases respectively due to $\pm$ 0.1 kms^{-1} change of the macroturbulence. Filled circle : log gf (1.52 V_{macro}) – log gf (1.62 V_{macro}), Filled triangle : log gf (1.52 V_{macro}) – log gf (1.42 V_{macro}). The top panels are for the KPNO J and H bands and the bottom panels are respectively for the Liege J and H bands.

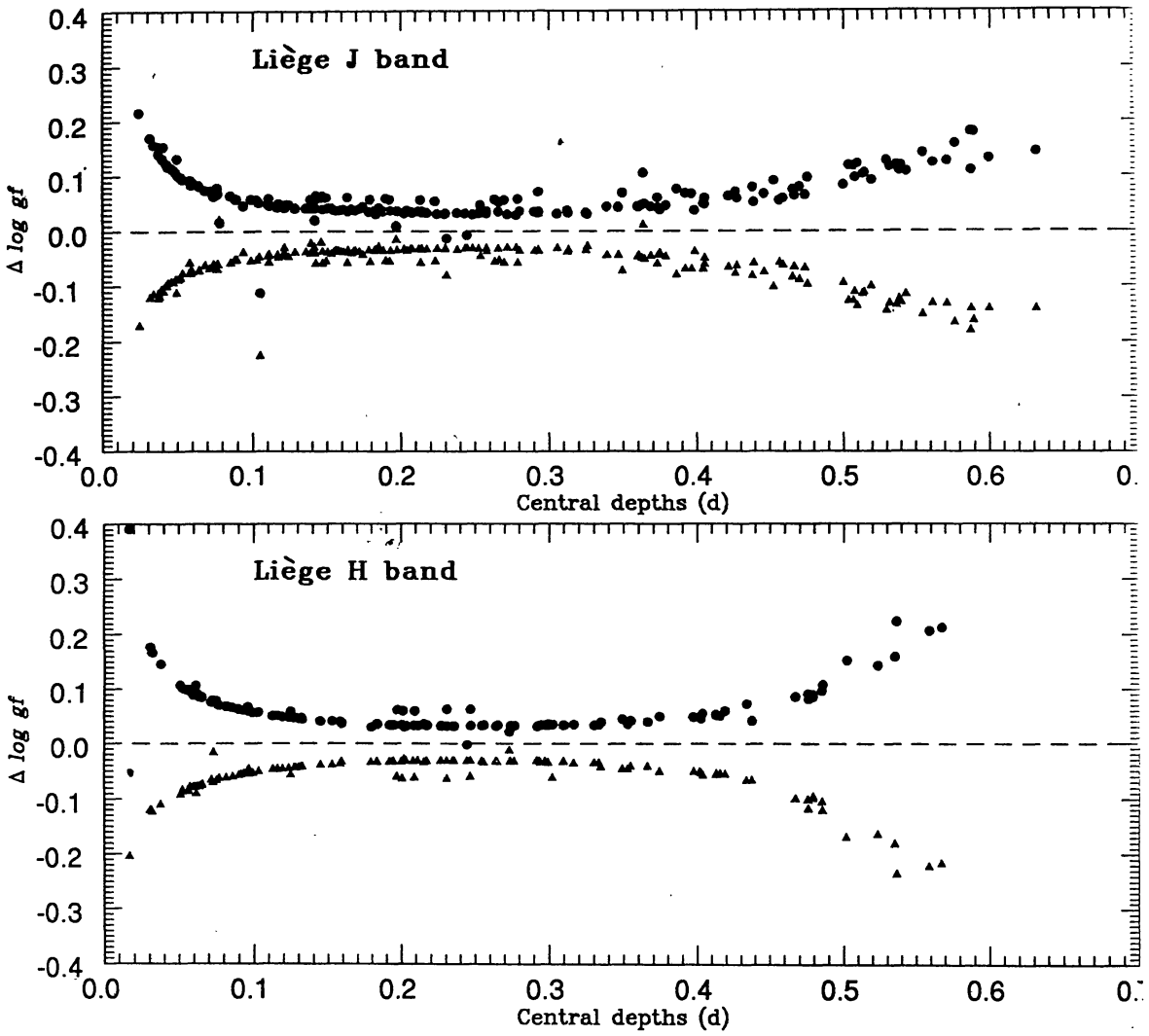

Figure 5. Log gf changes (Δ log gf) against observed central depths (d) due to ± 1% change in the continuum. Filled circle : log gf (d) – log gf (d + 0.01), filled triangle : log gf (d) – log gf (d – 0.01). The top panel is for Liège J band and the bottom panel is for Liège H band.

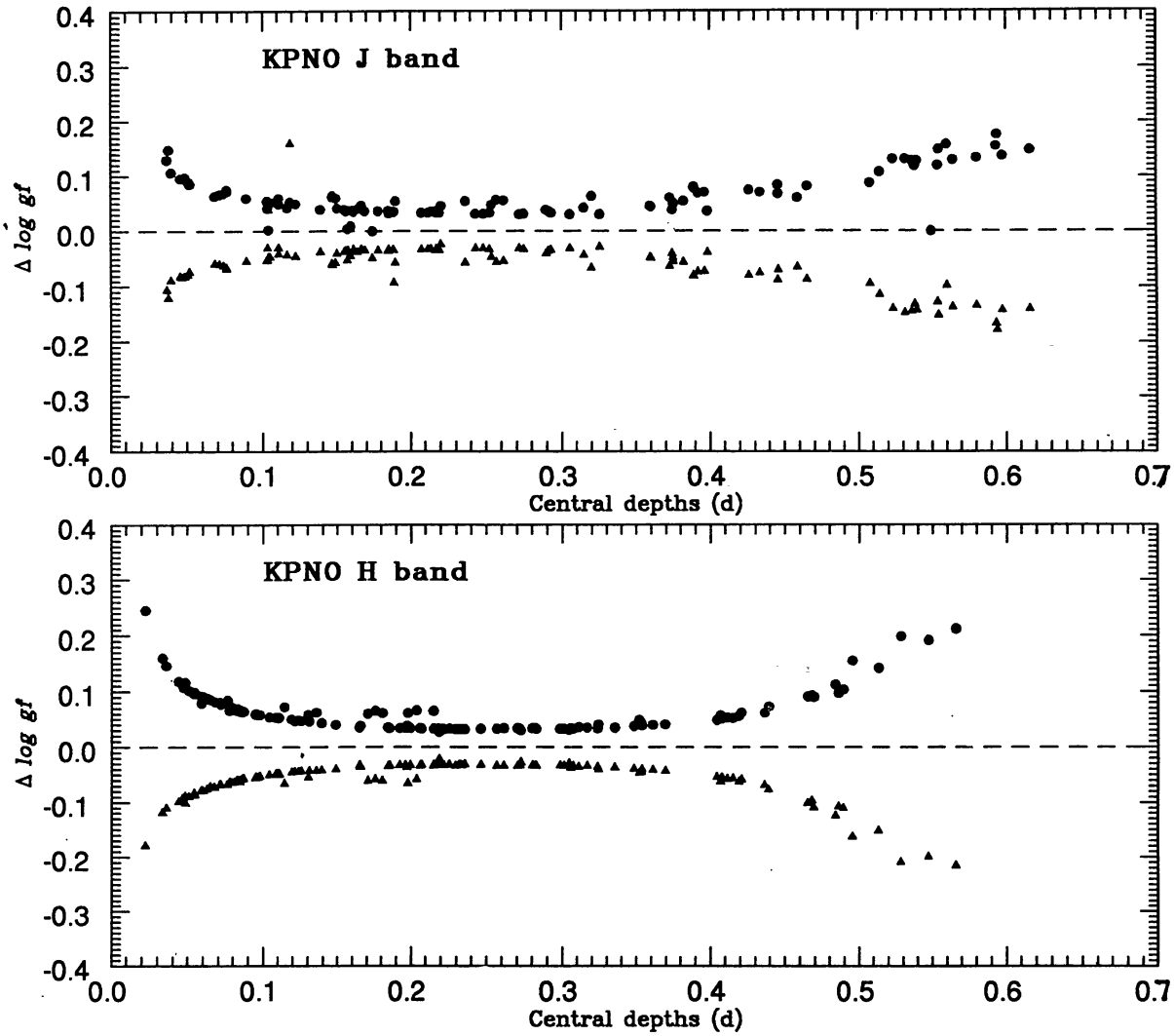

Figure 6. Same as in Fig. 5 but for the KPNO J band (top panel) and KPNO H band (bottom panel).

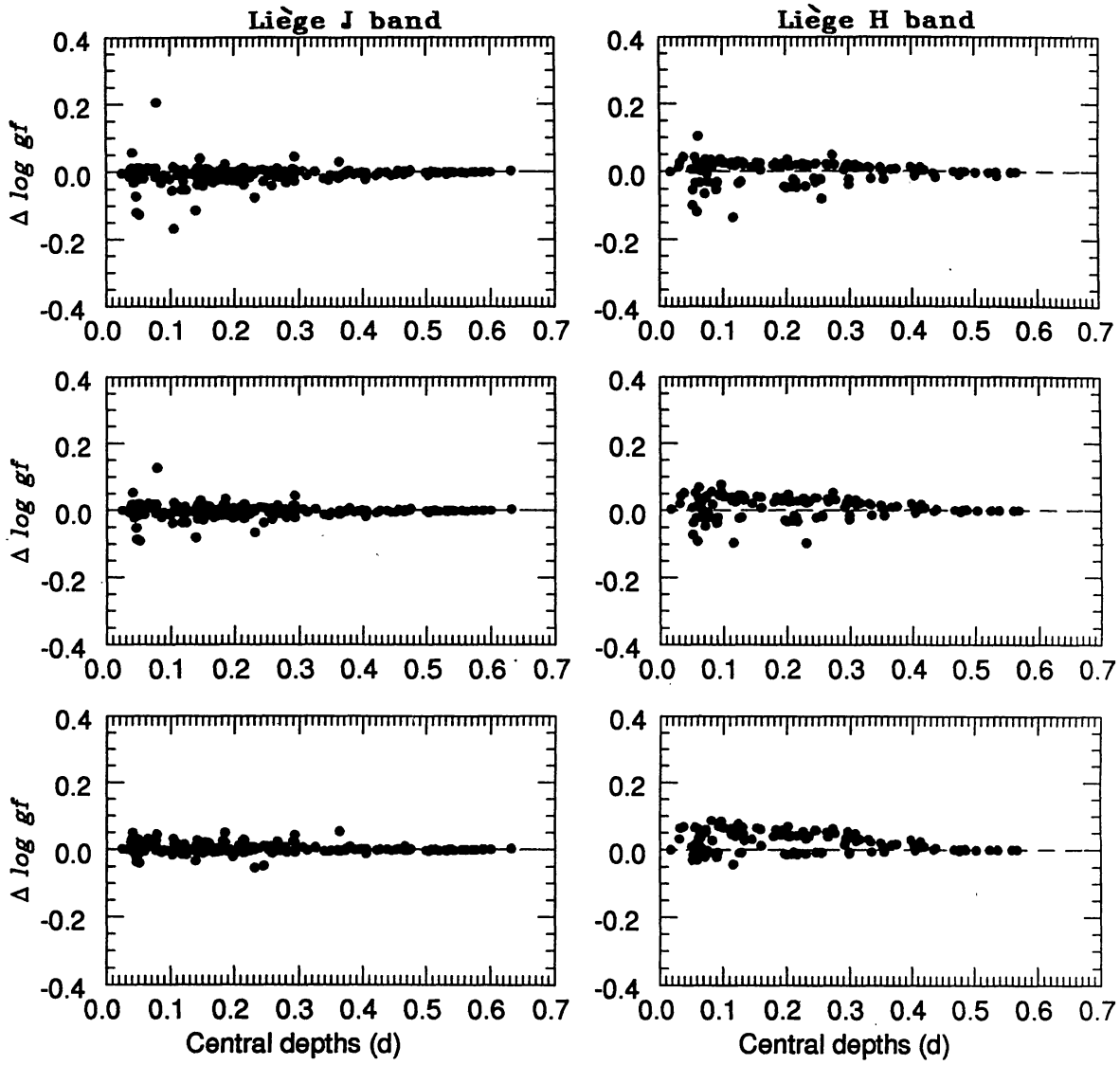

Figure 7. Log gf changes (Δ log gf) against observed central depths (d) for the Liège J and H bands respectively when enhancements factors of 1.5, 2.5 and 3.5 are used for γ_6. Top panels : enhancement by 3.5, middle panels : enhancement by 2.5 and bottom panels : enhancement by 1.5.

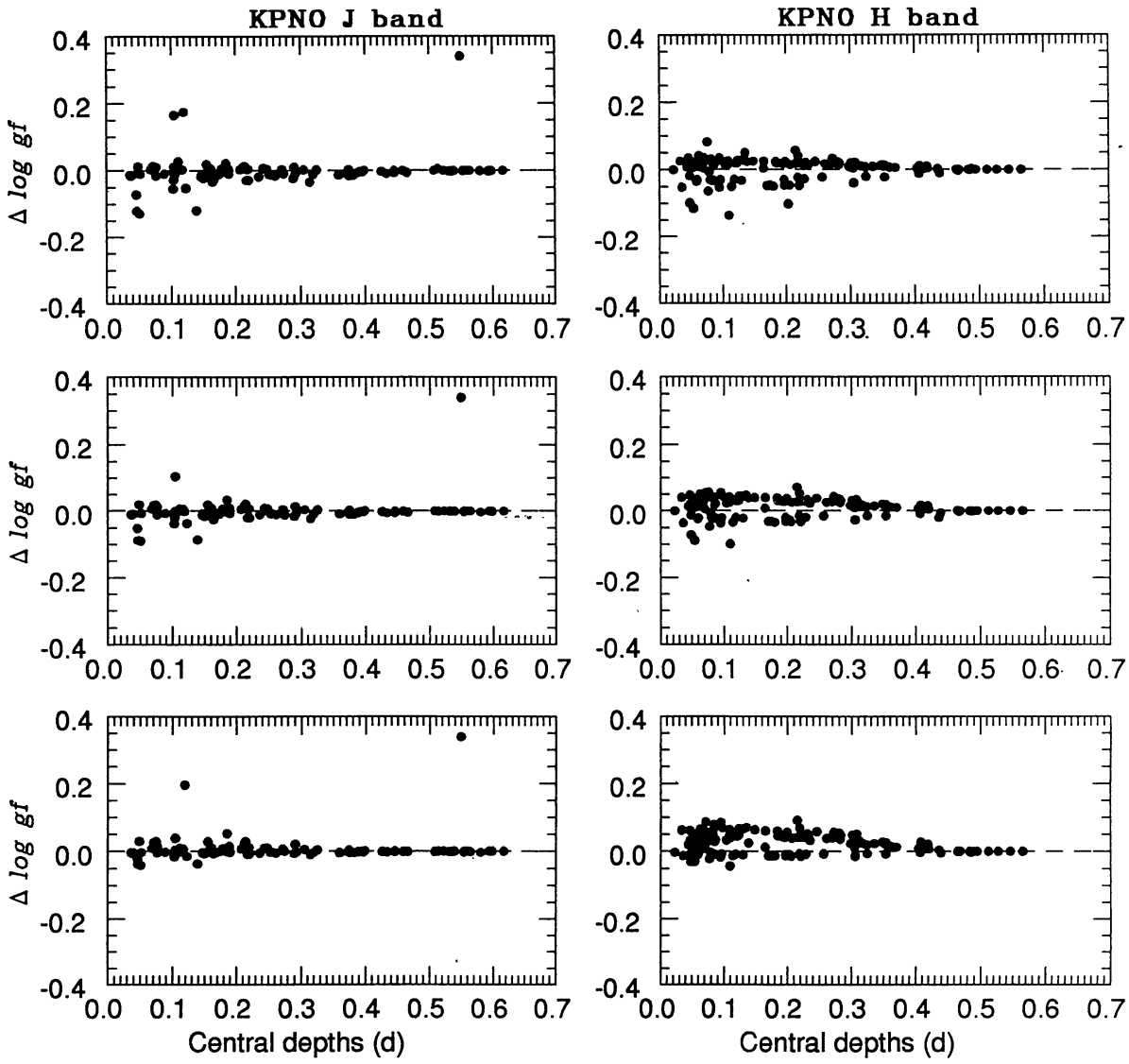

Figure 8. Same as in Fig. 7, but for the KPNO J and H bands

During the calculations, it was also found that there are certain lines for which the observed and the calculated central line depths can be matched but, a large portion of the profiles could not be fitted in spite of several attempts. Such lines are listed in Table 3 along with their central depths.

4. Conclusions

We feel that GK's method employed in the optical region can be applied to the infrared region as well. In Fig. 2a and Fig. 2b we show the log gf values obtained using the KPNO atlases plotted against the same obtained using Liège atlas for the J and H bands. The large scatter in Fig. 2a is due to the large number of lines in the Liège J band being blended with telluric lines. Figures 9 and 10 show the differences between RSB values and those derived by us against the lower excitation potential and central depths of the lines. It is seen that RSB values are mostly on the lower side except for a very few number of lines in the H band region. The log gf values as given by RSB as reliable ones for stellar spectroscopy are mostly from theoretical determinations and so large differences between our solar values and those given by RSB are not unexpected. Among the two sets of log gf values reported by us, we consider the one derived using the KPNO atlases as reliable to those derived using the Liège atlas.

Table 3. Lines showing peculiar behaviour.

Element	Excitation Potention (eV)	Wavelength (Laboratory) (Å)	Central Depths Liège	KPNO
J band				
Si I	6.09	10603.431	0.6048	0.6048
Si I	4.93	10749.384	0.6253	0.6253
Si I	4.93	10786.856	0.6055	0.6055
Si I	4.95	10827.090	0.6954	0.6954
Mg I	4.35	11828.171	0.6560	0.6557
Si I	4.93	11984.196	0.7106	0.6852
Si I	5.95	11991.570	0.6304	0.6391
Si I	4.95	12031.517	0.7174	0.7097
A1 I	3.14	13123.440	0.6839	0.6866
A1 I	3.14	13150.785	0.6538	0.6287

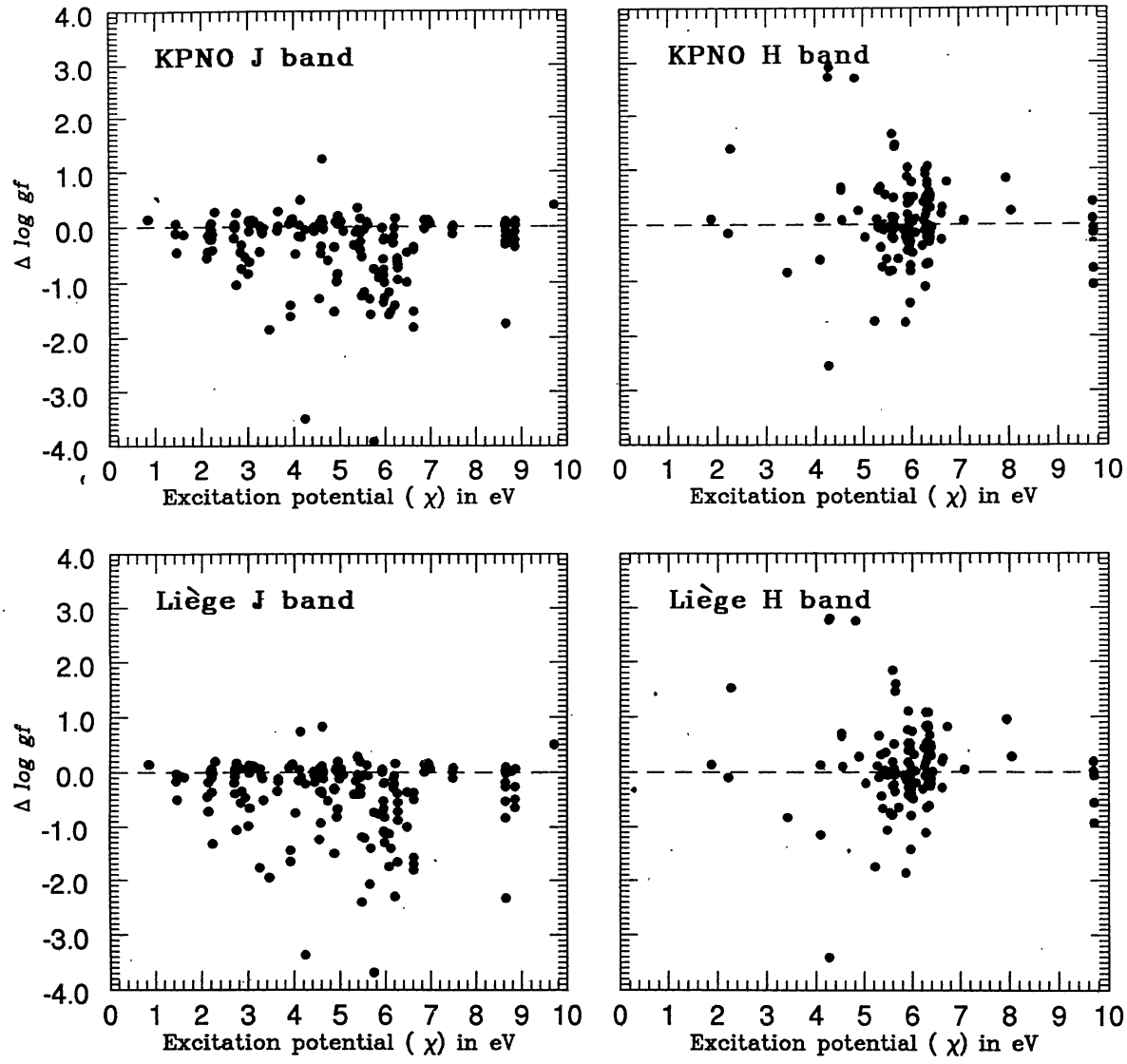

Figure 9. Differences in log gf (Δ log gf) between RSB and those derived by us against the lower excitation potential. The top panels are for KPNO J and H bands and the bottom panels are for Liege J and H bands.

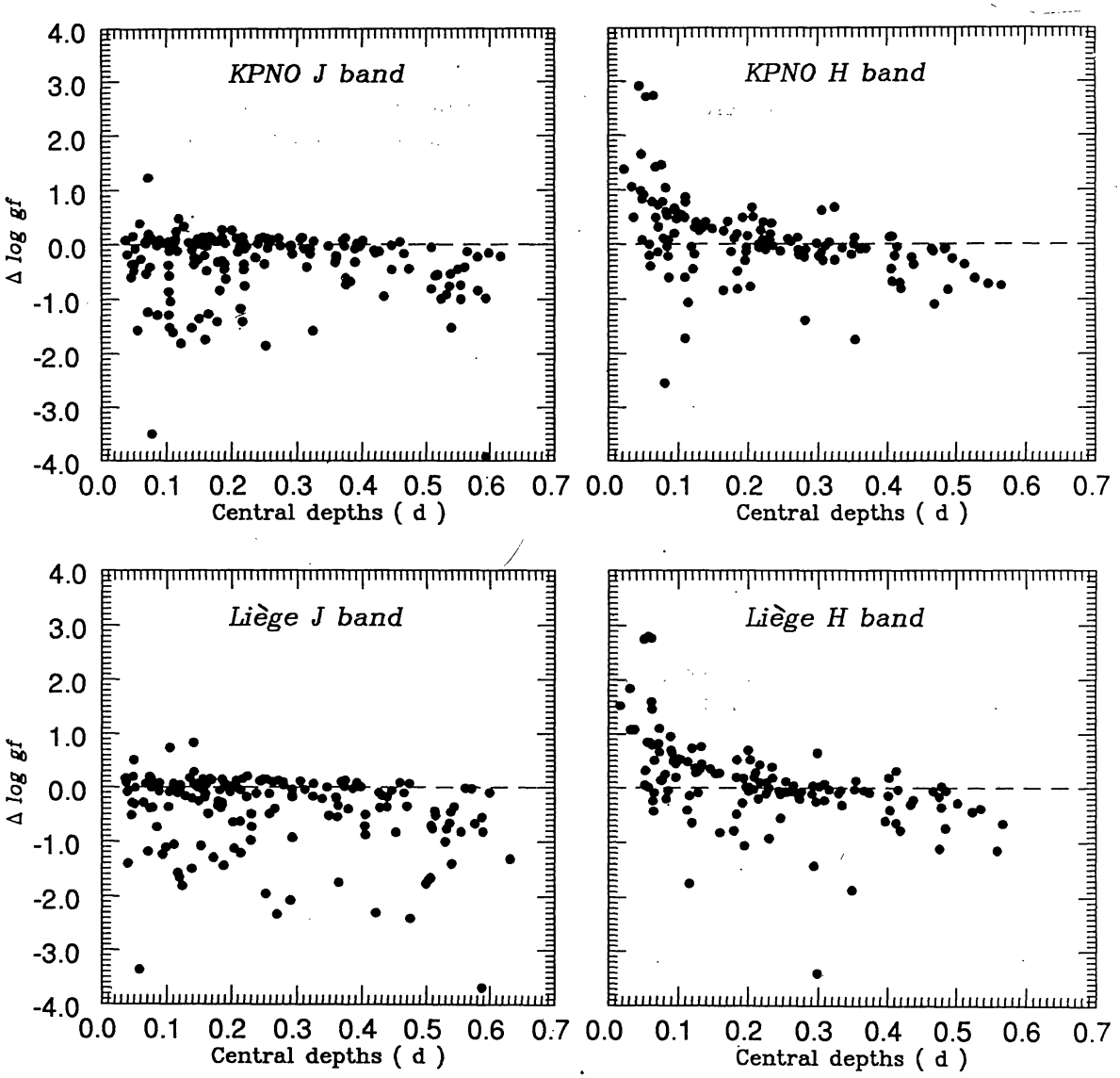

Figure 10. Differences in log gf (Δ log gf) between RSB and those derived by us against the observed central line depths (d). The top panels are for KPNO J and H bands and the bottom panels are for Liege J and H bands.

Acknowledgments

We express our sincere thanks to Professor L. Delbouille and Professor W. Livingston for providing us the digitised version of Liège-81 and KPNO-91 atlases respectively on magnetictapes. We are indebted to Mr J.S. Nathan of the Indian Institute of Astrophysics for sending us the KPNO-93 atlas. The authors also thank Professors K. Krishna Swamy, E. Biémont, J. Führ, R. Kostik, N. Grevesse, H. Holweger and A.J. Sauval for several invaluable suggestions which helped in a significant improvement of an earlier version of the manuscript. The financial support from the Department of Science and Technology, Government of India, is thankfully acknowledged.

References

Anders E., Grevesse N., 1989, Geochim. Cosmochim. Acta, 53, 197.

Baschek B., Holweger H., Tracing G., 1966, Abhandlungen aus der Hamburger Sternwarte VIII, 26.

Biémont E., Grevesse N., 1973, Atomic and Nuclear Data Tables, 12, No. 3.

Biémont E., Martin F., Quinet P., Zeippen C.J., 1994, A&A 283, 339.

Blackwell D.E., 1990, in Elements and the Cosmos, Edmunds M.J., Terlevich R.J. (eds.) Cambridge University Press, Cambridge, p. 28.

Blackwell D.E., Petford A.D., Shallis M.J., 1979b, MNRAS 186, 657.

Blackwell D.E., Petford A.D., Simmons G.J., 1982b, MNRAS 201, 595.

Blackwell D.E., Menon S.L.R., Petford A.D., 1982c, MNRAS 201, 603.

Blackwell D.E., Ibbeston P.A., Petford A.D., Wills R.B., 1976, MNRAS 177, 219.

Blackwell D.E., Ibbeston P.A., Petford A.D., Shallis M.J., 1979a, MNRAS 186, 633.

Blackwell D.E., Petford A.D., Shallis M.J., Simmons G.J., 1980, MNRAS 191, 445.

Blackwell D.E., Petford A.D., Shallis M.J., Simmons G.J., 1982a, MNRAS 199, 43.

Blackwell D.E., Menon S.L.R., Petford A.D., Shallis M.J., 1982d, MNRAS 201, 611.

Chmielewski Y., 1979, Publ. Observ. Geneva, Ser. B., Fasc 7.

Delbouille L., Neven L., Roland C., 1973, Photometric Atlas of the Solar Spectrum from λ 3000 to λ 10,000, Institut d' Astrophysique de l'Universite de Liège, Belgique.

Delbouille L., Roland G., Brault J.W., Testerman L., 1981, Photometric Atlas of the Solar Spectrum from 1850 to 10,000 cm^{-1}, NOAO, Tucson, Arizona.

Führ J., 1987, in Elemental Abundance Analyses, Adelman S.J., Lanz T. (ed.) Institut d' Astronomie de l'Université de Lausane, Switzerland, p. 173.

Grevesse E., Noels N., 1993, in Origin and Evolution of the Elements, Prantzos N., Vangioni-Flam E., Cassé M. (eds.) Cambridge University Press, Cambridge, p. 15.

Gurtovenko E.A., Kostik R.I. 1981, A&AS, 46, 239.

Gurtovenko E.A., Kostik R.I. 1982, A&AS, 47, 193.

Gurtovenko E.A., Kostik R.I., 1989, Fraunhofer Spectrum and the System of Oscillator Strengths, Naukova Dumka, Kiev.

Holweger H., Müller E.A., 1974, Sol. Phys. 39, 19.

Holweger H., Heise C., Kock M., 1990, A&A 232, 510.

Holweger H., Bard A., Kock A., Kock M., 1991, A&A 249, 545.

Keenan F.P., Brown P.J.F., Dufton P.L., Holmgren D.E., 1990, in Atomic. Spectrum and Oscillator Strengths for Astrophysics and Fusion Research, Hansen J.E. (ed.) Amsterdam, North Holland,. p. 44.

Kostik R.J., Shchukina N.G., Rutten R.S., 1996, A&A 305, 325.

Kurucz R.L., Peytremann E., 1975, Smithsonian Astrophys. Obs., Special Rep. 362.

Kurucz R.L., 1991, Magnetic tape with atomic data.

Kurucz R.L., 1994, CD - ROM No.1.

Livingston W., Wallace L., 1991, An Atlas of the Solar Spectrum in the Infrared from 1850 to 9000 cm^{-1} (1.1 to 5.4 μm), Techn. Rep. # 91 - 001, National Solar Obs., Tucson, Az.

Nave G., Johansson S., Learner R.C.M., Thorne A.P., Brault J.W., 1984, ApJS, 94, 221.

Peytremann E., Baschek B., Holweger H., Traving G., 1967, Un programme FORTRAN d'analyse quantitative de spectres stellaires, Rapport Interne, Observatoire de Geneva.

Ramsauer J., Solanki S.K., Biémont E., 1995, A&AS 113, 71.

Rogers F., Iglesias C.A., 1995, in Astrophysical application of powerful new atomic databases, Adelman S.J., Wiese W.L. (eds.) San Francisco, ASP, ASP conf. Series, Vol. 78, p.31.

Solanki S.K., Biémont E., Murset U., 1990 A&AS 83, 307.

Stalin C.S., Sinha K., Sanwal B.B., 1996 (in press).

The Opacity Project Volume 1, 1995, The Opacity Project Team (eds.) Institute of Physics Publishing, Bristol and Philadelphia, ISBN 0 7503 02887.

Thévenin F., 1989, A&AS 77, 137.

Thévenin F., 1990, A&AS 82, 179.

Unsöld A., 1955, Physik der Sternatmospharen, Aufl. Berlin - Gottingen - Heidelberg, Springer.

Wallace L., Hinkle K., Livingston W., 1993, An Atlas of the Photospheric Spectrum from 8900 to 13600 cm^{-1} (7350 to 11230 Å), Techn. Rep. # 93-001, National Solar Obs., Tucson, Az.

Wallace L., Livingston W., Bernath P., 1994, An Atlas of the Sunspot Spectrum from 470 to 1233 cm^{-1} (8.1 to 21 μm) and the Photospheric Spectrum from 460 to 630 cm^{-1} (16 to 22 μm), Tech, Rep. # 1994-01, National Solar Obs., Tucson, Az.